High power diode laser modification of the wettability characteristics of an Al_2O_3/SiO_2 based oxide compound for improved enamelling

J. Lawrence [a,*], L. Li [a], J.T. Spencer [b]

[a] *Manufacturing Division, Department of Mechanical Engineering, University of Manchester Institute of Science and Technology (UMIST), Manchester, M60 1QD, UK*
[b] *Research & Technology, B709, BNFL, Springfields Works, Salwick, Preston, Lancashire, PR4 0XJ, UK*

Abstract

High power diode laser (HPDL) surface melting of a thin layer of an amalgamated Al_2O_3/SiO_2 oxide compound (AOC) resulted in significant changes in the wettability characteristics of the material. This behaviour was identified as being primarily due to: (1) the polar component of the AOC surface energy increasing after laser melting from 2.0 to 16.2 mJ m^{-2}, (2) the surface roughness (Ra) of the AOC decreasing from 25.9 to 6.3 μm after laser melting and (3) the relative surface oxygen content of the AOC increasing by 36% after laser melting. HPDL melting was consequently identified as affecting a decrease in the enamel contact angle from 118° prior to laser melting to 33° after laser melting, thus allowing the vitreous enamel to wet the AOC surface. The effective melt depth for such modifications was measured as 50 to 125 μm. The morphological, microstructural and wetting characteristics of the AOC were determined using optical microscopy, scanning electron microscopy, energy disperse X-ray analysis, X-ray diffraction techniques and wetting experiments by the sessile drop technique. The work has shown that laser radiation can be used to alter the wetting characteristics of the AOC only when surface melting occurs. © 1999 Published by Elsevier Science S.A. All rights reserved.

Keywords: High power diode laser (HPDL); Vitrification; Melting; Enamel; Adhesion; Surface energy; Wettability

1. Introduction

Both scientists and engineers alike have a great interest in understanding the interfacial phenomena between vitreous enamels and ceramic materials, since in many practical applications where vitreous enamels are fired onto ceramic substrates, the performance of the article is directly linked to the nature of the enamel–ceramic interface. Many studies to investigate these phenomena have been carried out; however, they have been principally concerned with the wettability of zirconia and other oxide ceramics on metals [1–5] as well as the adhesion of silicone sealants to aluminium [6] and the coating of aluminium alloys with ceramic materials [7,8]. The interfacial mechanisms investigated have cen-

tred principally around the thermodynamic criterion [2,3,5], the electronic theory [4] and the occurrence of oxidation [1,9].

At present, very little work has been published with regard to the use of lasers for altering the surface properties of materials in order to improve their wettability characteristics. Notwithstanding this, it is recognised within the currently published work that laser irradiation of material surfaces can affect its wettability characteristics. Previously Zhou et al. [7,8] have carried out work on laser coating of aluminium alloys with ceramic materials (SiO_2, Al_2O_3, etc.), reporting on the well documented fact that generated oxide layers often promote metal/oxide wetting. Bahners et al. [10,11], have observed and comprehensively detailed the changes in technical properties of various textile fibres, including adhesion and wetting properties, with a view to developing an alternative to the conventional meth-

* Corresponding author. Tel.: +44-161-200-3816; fax: +44-161-200-3803.
E-mail address: j.lawrence@stud.umist.ac.uk (J. Lawrence)

ods of chemical agents addition or wet-chemical pre-processing. However, the reasons for these changes with regard to changes in the material's surface tension are not reported.

This paper describes a technique whereby a high power diode laser (HPDL) beam was used to alter the wettability characteristics of an amalgamated alumina/silica-based oxide compound (AOC) mix to facilitate improved enamelling. Indeed, such a process has been employed by the authors to enable the sealing, by means of laser enamelling, of ceramic tile grouts [12].

2. Experimental procedures

2.1. The amalgamated oxide compound grout and enamel

The AOC consisted of mixed vitrifiable oxide powders such as chamotte (mainly SiO_2 (53 wt%) and Al_2O_3 (42 wt%)), Fe_2O_3, MgO, ZrO_2 and ZnO. The oxide powders were sieved to ensure a particle size of less than 75 μm, then thoroughly mixed together to ensure homogeneity, along with approximately 50 wt.% diluted sodium silicate solution so as to form a manageable paste. The AOC was then pasted onto an ordinary Portland cement (OPC) substrate to a thickness of 2 mm and allowed to cure at room temperature for 12 h. The composition of the enamel consisted mainly of the following: SiO_2, B_2O_3, Na_2O, Mn, F and small quantities of Ba, Al_2O_3 and Ni, whilst the powder size was less than 75 μm. The enamel frit paste was allowed to cure at room temperature for 1–2 h and then irradiated immediately with the HPDL beam.

2.2. Laser processing procedure

The laser used in the study was a surgical HPDL (Diomed), emitting at 810 ± 20 nm and operating in the CW mode with rated optical powers ranging from 0 to 60 W. The laser beam was delivered to the work area by means of an optical fibre 4 m long, and of 600 μm core diameter, the end of which was connected to a 2:1 focusing lens assembly mounted on the z-axis of a three-axis CNC gantry table. The AOC was irradiated using the defocused high-order mode HPDL beam with a beam spot diameter of 1.75 mm and laser powers (measured at the workpiece using a Power Wizard power meter) of 20–55 W. The set compound was then irradiated using the HPDL and immediately pasted over with a thin layer (250 μm) of commercially available enamel frit (Ferro) which, in order to form a manageable paste, was mixed with 20 wt% white spirit. Fig. 1 illustrates the laser processing experimental arrangement, where the defocused laser beam was fired across the surfaces of the AOC and the vitreous enamel

by traversing the samples beneath the laser beam using the x- and y-axis of the CNC gantry table at speeds ranging from 300 to 480 mm min^{-1}, whilst 3 l min^{-1} of coaxially blown O_2 assist gas was used to shield the laser optics.

2.3. Wetting and surface energy characterisation procedure

In order to analyse the laser treated specimens, they were sectioned with a Struers cutting machine using a diamond rimmed cutting blade, and then polished using cloths and diamond suspension pastes down to 3 μm. The sectioned samples were then examined using optical microscopy, scanning electron microscopy (SEM), energy disperse X-ray analysis (EDX) and X-ray diffraction (XRD) techniques.

To examine the wetting and surface energy characteristics of the AOC two sets of wetting experiments were conducted. The first set of experiments were to simply determine the contact angle between the enamel and the AOC before and after laser melting. The second set of experiments were control experiments carried out using the sessile drop technique with a variety of liquids with known surface energy properties in order to quantify any surface energy changes in the AOC resulting from laser irradiation.

The enamel–AOC wetting experiments were carried out in normal atmospheric conditions with molten droplets of the enamel (600°C). The temperature of the enamel throughout the experiments was measured using a Cyclops infrared pyrometer. The droplets were released onto the surface of the AOC (treated and untreated) from the tip of a micropipette, with the resultant volume of the drops being approximately 15×10^{-3} cm^3. Profile photographs of the sessile enamel drop were obtained for every 60°C fall in temperature of the molten enamel drop, with the contact angle subsequently being measured.

The sessile drop control experiments between the AOC and test liquids were carried out using: human
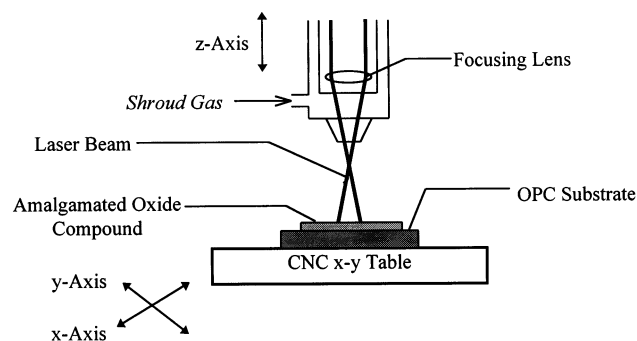

Fig. 1. Schematic of the experimental set-up for the HPDL treatment of an amalgamated oxide compound and a vitreous enamel.

Table 1
Total surface energy (γ_{lv}) and the dispersive (γ_{lv}^d) and polar (γ_{lv}^p) components for the selected test liquids [6][a]

Liquid	γ	γ_{lv}^d	γ_{lv}^p
Human blood	47.5	11.2	36.3
Human blood plasma	50.5	11.0	39.5
Glycerol	63.4	37.0	26.4
4-Octonol	27.5	7.4	20.1

[a] Values are in mJ m^{-2}.

blood, human blood plasma, glycerol and 4-octanol. The test liquids, along with their total surface energy (γ_2) as well as the dispersive (γ_{lv}^d) and polar (γ_{lv}^p) components, are detailed in Table 1. The experiments were conducted in normal atmospheric conditions at a temperature of 20°C with the temperature of the liquids themselves throughout the experiments also being maintained at 20°C. The droplets were released onto the surface of the test substrate materials (treated and untreated) from the tip of a micropipette, with the resultant volume of the drops being approximately 6×10^{-3} cm^3. Each experiment lasted for 3 min with profile photographs of the sessile drops being obtained every minute, with the contact angle subsequently being measured.

3. Results and discussion

3.1. Microstructural and morphological effects of laser radiation on the amalgamated oxide compound

The oxide compounds of the amalgamation were bound together by mixing with 50 wt% diluted sodium silicate solution. Sodium silicate solution (waterglass) is a viscous colourless solution of colloidal sodium silicate. It is a silica containing aqueous solution that, when combined with other solutions such as the amalgamated oxide compound, forms a gel-like mass of silicate hydrate. Such a mass remains soft and malleable until it is exposed to CO_2 gas, either by means of a gas jet or through contact with the atmosphere [17]. But, exposure of the hardened mass to water results in a reversing of the process and the mass returns to a gel-like state.

The fact that the AOC in an unheated state is hydraulically bonded, as opposed to chemically bonded, combined with the retention of chemical and mechanical water (that is water that is bonded into the materials matrix and additional free-water respectively) means that the hardened mass will rehydrate when exposed to water [17,18]. Heating of the hardened AOC mass fires the waterglass (similar to that of a ceramic material) [17], increasing its strength and enabling it to withstand water exposure. Thus, heating of the AOC is similar in effect to the firing of ceramics, in that the heating causes gradual ceramic 'sintering' of the materials; generally bonding together and stabilising the substances [17,19]. As such, exposure of the AOC to laser radiation results in rapid heating of the surface, for most materials typically 10^3 to 10^5 K s^{-1} [20]. This leads to the sintering of the AOC surface with the removal of the pores between the starting particles of the compound, combined with growth together and strong bonding between adjacent particles [21], thus, a much more consolidated surface is created. Indeed, surface roughness measurements revealed that the surface roughness had decreased from an Ra value of 25.9 μm before laser melting, to 6.3 μm after laser melting. Also, it was found that heating of the AOC above 100°C resulted in sufficient pyrochemical changes to prevent any rehydration.
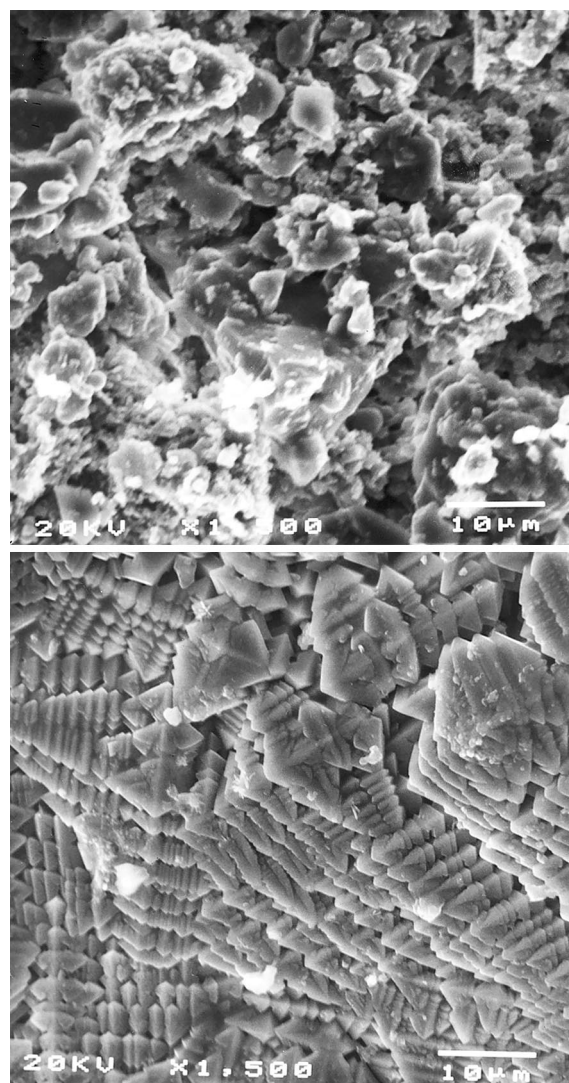

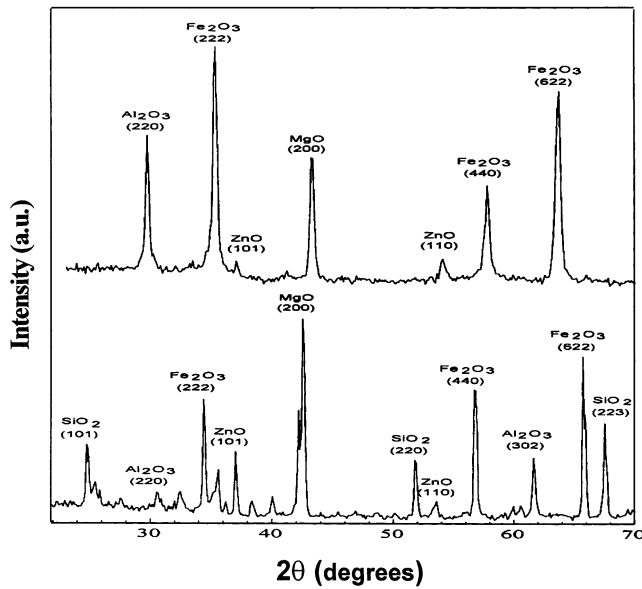Fig. 2. Typical SEM surface images of the AOC (a) untreated and (b) laser treated.

Fig. 3. XRD analysis of the AOC before (bottom) and after (top) laser treatment.

From Fig. 2(a) it can be seen clearly that before laser treatment the surface of the AOC appears coarse, with individual crystals of the constituent components being clearly discernible. After laser treatment (Fig. 2(b)) there is more surface ordering, with the surface appearing cellular-dendritic, showing that fusion of the individual particulates has occurred. Such a solidification structure is indicative of rapidly solidified microstructures [22]. Moreover, an XRD analysis of the AOC surface before and after laser treatment (Fig. 3) revealed that, on the whole, the phases present within the laser treated region were the same, however, their proportions were different. In particular, after laser treatment it was not possible to detect any SiO_2 whilst the Al_2O_3 was depleted. But, an EDX analysis showed that Si and Al were still present in similar proportions on the AOC surface before and after laser treatment. This indicates that partial laser vitrification of the AOC surface has occurred due to the fact that these materials are glass forming elements, and as such, vitrified when irradiated. Additionally, it is important to note that the peaks in Fig. 3 which are unmarked, for ease of analysis since they are not of direct interest, are likely to be mullite 121 and 220, which provides diffraction peaks in the range 35 to 40°. Further, some formation of spinel ($MgAl_2O_4$) would perhaps be expected; however, this was not detected.

3.2. Laser induced wettability and surface energy characteristics of the amalgamated oxide compound

3.2.1. Contact angle and wettability

When a drop of liquid is placed on a solid surface it may remain as a spherical drop, or spread to cover (wet) the solid surface [13]. The angle with which the liquid subtends the solid is known as the contact angle. In practice, if the contact angle is greater than 90° then the liquid does not wet the solid and no adhesion occurs [13]. Once irradiated by the HPDL beam the enamel powder melts, transforming to a liquid phase. As such, the process of the bonding of the enamel to the AOC substrate is determined by the wettability of the two component parts. The index of this effect is the contact angle θ, which the liquid subtends with the solid. θ is related to the solid and liquid surface energies, γ_{sv} and γ_{lv}, and the solid–liquid interfacial energy γ_{sl}, through the principle of virtual work expressed by the rearranged Young's equation:

$$\cos \theta = \frac{\gamma_{sv} - \gamma_{sl}}{\gamma_{lv}} \tag{1}$$

Clearly, to achieve wetting γ_{sv} should be large, while γ_{sl} and γ_{lv} should be small. Hence liquids of a lower surface tension will always spread over a solid surface of higher surface tension in order to reduce the total free-energy of the system [14]. This phenomenon is due to fact that the molecular adhesion between solid and liquid is greater than the cohesion between the molecules of the liquid [13].

The adhesion energy of a liquid to a solid surface (the work of adhesion) W_{ad}, is given by the Young–Dupre equation:

$$W_{ad} = \gamma_{lv}(1 + \cos \theta) \tag{2}$$

It is important to consider also the influence of the substrate surface roughness on the wetting contact angle. Rough grooves on a surface, which may contribute to the influence of contact angles, can be categorised as either radial or circular grooves. Any practical rough surface can be represented by a combination of these two cases [23]. In fact two roughness parameters can be defined: the Wenzel type, D_R [24] and the Cassie/Baxter type, F_R [25]. In the case that wetting spreads radially, as is the likely case with the AOC, then the resulting radial contact angle, θ_{rad}, is related to the theoretical contact angle, θ_{th}, by

$$\cos \theta_{rad} = D_R(1 - F_R) \cos \theta_{th} - F_R \tag{3}$$

According to Neumann [15], only if F_R is equal to zero, then a model similar to that for heterogeneous solid surfaces can be developed in order to account for surface irregularities, being given by Wenzel's equation:

$$r(\gamma_{sv} - \gamma_{sl}) = \gamma_{lv} \cos \theta_w \tag{4}$$

where r is the roughness factor defined as the ratio of the real and apparent surface areas and θ_w is the contact angle for the wetting of a rough surface. It is important to note that Wenzel's treatment is only effective at the position of wetting triple line [23]. Nevertheless, Eq. (4) shows clearly, the influence of surface

roughness on the contact angle is to cause an increase in the contact angle. Thus, the smoother the contact surface is, then the smaller the contact angle will be.

An optical micrograph of a sessile drop of enamel (20°C) placed on the surface of the AOC before (a) and after (b) laser irradiation with the contact angle superimposed is shown in Fig. 4. The experimental results showed that throughout the period of cooling of the enamel, from the molten state at 600°C to the solid state at room temperature, no discernible change in the magnitude of the contact angle took place during the time of the experiments. This observation indicates that thermodynamic equilibrium was established at the solid–liquid interface at the outset of the experiment [26].

Fig. 4 shows clearly that prior to laser melting it was not possible to fire the enamel onto the surface of the AOC since the contact angle was measured as 118°, and as such would prevent the enamel from wetting the AOC surface. Indeed, laser interaction with the enamel when placed on the untreated AOC surface simply resulted in the 'balling' of the enamel; the formation of small spheres approximately the diameter of the laser beam itself [27,28].

One explanation for the fact that laser melting of the AOC is necessary so that the enamel completely wets and adheres to the surface of the AOC is that the surface resulting from the laser melting is significantly smoother, with an Ra value of 25.9 μm compared with 6.3 μm. Similar results were obtained by Nicolas et al. [29], who observed that excimer laser treatment of a ZrO_2 ceramic resulted in a smoother surface. Thus, according to Eq. (3), will intrinsically affect a reduction in the contact angle (Table 2). Indeed, Fig. 5 shows clearly the effect of the laser treated AOC surface roughness on the contact angle. For experimental purposes the liquid used was glycerol. Such results are in accord with those obtained by Feng et al. [30], who noted that contact angle was inversely proportional to surface roughness.

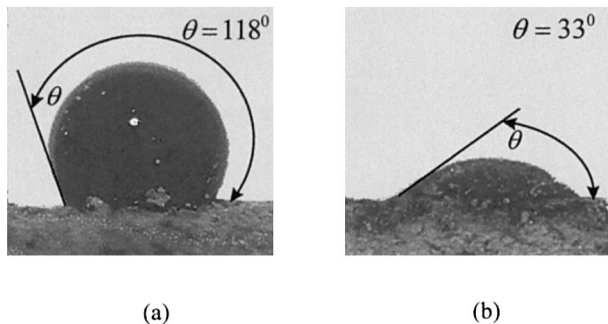Additionally, wetting will have certainly been influenced by the increase in the oxygen content of the AOC

Table 2
Measured surface energy values for the AOC before and after HPDL irradiation

Characteristic	Untreated AOC	HPDL treated AOC
Contact angle (°)	118	33
Surface roughness (Ra, μm)	25.9	6.3
Relative oxygen content (%)	28	39
Dispersive component, (γ_{sv}^{d}) (mJ m^{-2})	84.2	89.0
Polar component, (γ_{sv}^{p}) (mJ m^{-2})	2.0	16.2

surface as a result of the laser treatment, since this interaction is known to increase the likelihood of wetting [1,9]. Indeed, by mounting cross-sectioned samples of the untreated and laser treated AOC next to each other, and examining them both simultaneously by means of EDX, it is possible to determine the relative element content of oxygen near to the surface. Values of 28 and 39% for the untreated and laser treated AOC respectively were obtained from such an EDX analysis which probed to a depth of approximately 1 μm below the surface of both samples (Table 2). As one can see, an increase of 36% in the amount of oxygen due to the oxidisation on the laser treated surface of AOC has occurred, indicating that oxygen enrichment of the laser treated AOC surface is active in promoting wetting and bonding.

3.2.2. Amalgamated oxide compound surface energy and its dispersive/polar character

The intermolecular attraction which is responsible for surface energy, γ, results from a variety of intermolecular forces whose contribution to the total surface energy is additive [16]. The majority of these forces are functions of the particular chemical nature of a certain material, and as such the total surface energy comprises of γ^{p} (polar or non-dispersive interaction) and γ^{d} (dis-

Fig. 4. Contact angles for the enamel on (a) the untreated surface of the AOC, (b) laser treated surface of the AOC.
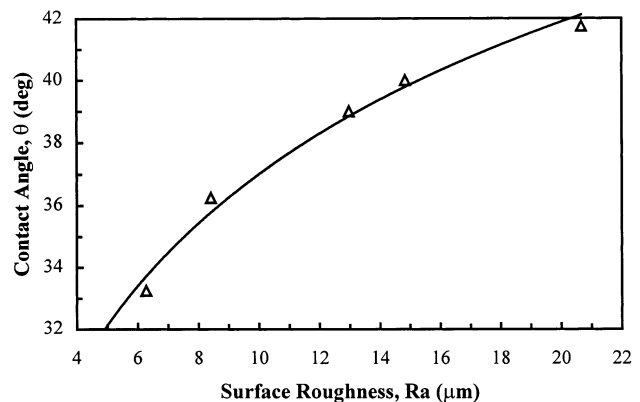

Fig. 5. Relationship between HPDL treated AOC contact angle (θ) and surface roughness (Ra).
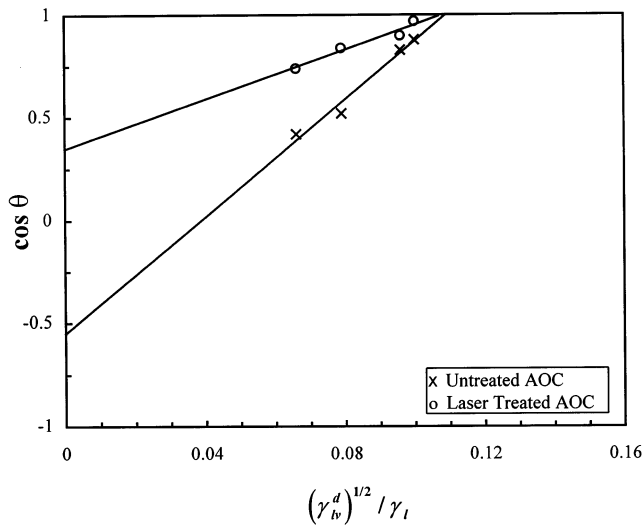
Fig. 6. Plot of $\cos\theta$ against $(\gamma_{lv}^d)^{1/2}/\gamma_{lv}$ for the AOC in contact with the wetting test control liquids.

persive component; since van der Waals forces are present in all systems regardless of their chemical nature). Therefore, the surface energy of any system may be described by [16]

$$\gamma = \gamma^d + \gamma^p \tag{5}$$

Similarly, W_{ad} can be expressed as the sum of the different intermolecular forces that act at the interface between the solid–liquid interface [31]:

$$W_{ad} = W_{ad}^d + W_{ad}^p = 2(\gamma_{sv}^d\gamma_{lv}^d)^{1/2} + 2(\gamma_{sv}^p\gamma_{lv}^p)^{1/2} \tag{6}$$

By equating Eq. (6) with Eq. (2), the contact angle for solid–liquid systems can be related to the surface energies of the respective liquid and solid by

$$\cos\theta = \frac{2(\gamma_{sv}^d\gamma_{lv}^d)^{1/2} + 2(\gamma_{sv}^p\gamma_{lv}^p)^{1/2}}{\gamma_{lv}} - 1 \tag{7}$$

It is possible to adequately estimate the dispersive component of the AOC surface energy γ_{sv}^d by using Eq. (7), and plotting the graph of $\cos\theta$ against $(\gamma_{lv}^d)^{1/2}/\gamma_{lv}$. Thus the value of γ_{sv}^d is estimated by the gradient $(= 2(\gamma_{sv}^d)^{1/2})$ of the line which connects the origin ($\cos\theta = -1$) with the intercept point of the straight line ($\cos\theta$ against $(\gamma_{lv}^d)^{1/2}/\gamma_{lv}$) correlating the data point with the abscissa at $\cos\theta = 1$ [16]. Fig. 6 shows the best-fit plot of $\cos\theta$ against $(\gamma_{lv}^d)^{1/2}/\gamma_{lv}$ according to Eq. (7) for the untreated and laser treated AOC–experimental control liquids system. Comparing the ordinate intercept points of the untreated and laser treated AOC–liquid systems, it can be seen clearly from Fig. 6 that for the untreated AOC–liquid systems the best-fit straight line intercepts the ordinate closer to the origin. This observation indicates that, in principle, dispersion forces act mainly at the AOC–liquid interfaces resulting in poor adhesion [16,31]. In contrast, Fig. 6 shows that the best-fit straight line for the laser treated AOC–liquid systems intercepts the ordinate considerably higher above the origin. This result is indicative of the action of polar forces across the interface, in addition to dispersion forces, hence improved wettability and adhesion is promoted [16,31].

It is not possible to determine the value of the polar component of the AOC surface energy γ_{sv}^p directly from Fig. 6, because the intercept of the straight line ($\cos\theta$ against $(\gamma_{lv}^d)^{1/2}/\gamma_{lv}$) is at $2(\gamma_{sv}^p\gamma_{lv}^p)^{1/2}/\gamma_{lv}$, and thus only refers to individual control liquids and not the control liquid system. However, it has been established that the entire amount of the surface energies due to dispersion forces either of the solids or the liquids are active in the wettability performance [16,32]. Thus it is possible to calculate the dispersive component of the work of adhesion, W_{ad}^d from Eq. (6). The results reveal that for each particular control liquid in contact with both the untreated and laser treated AOC surfaces, W_{ad} can be correlated with W_{ad}^d by the relationship

$$W_{ad} = aW_{ad}^d + b \tag{8}$$

Also, for the control test liquids used, a linear relationship between the dispersive and polar components of the control test liquids surface energies has been deduced which satisfies the equation

$$(\gamma_{lv}^p)^{1/2} = 1.3(\gamma_{lv}^d)^{1/2} + 1.15 \tag{9}$$

By introducing Eq. (8) into Eq. (6) and rearranging, then

$$W_{ad}^p = (a-1)W_{ad}^d + b \tag{10}$$

By combining Eq. (10) with Eq. (6) and differentiating with respect to $(\gamma_{lv}^d)^{1/2}$, then the following can be derived:

$$(\gamma_{sv}^p)^{1/2} = \frac{(\gamma_{sv}^d)^{1/2}(a-1)}{1.3} \tag{11}$$

From a plot of Eq. (10), a can be determined for the untreated and laser treated AOC (1.2 and 1.7 respectively). Since γ_{sv}^d has already been determined for the untreated and laser treated AOC from Fig. 6, then it is possible to calculate γ_{sv}^p for untreated and laser treated AOC using Eq. (11).

Table 2 details the values determined for γ_{sv}^d and γ_{sv}^p for both the untreated and laser treated AOC. Clearly the HPDL melting of the surface of the AOC leads to a reduction in the total surface energy γ_{sv}, whilst increasing the polar component of the surface energy γ_{sv}^p, thus improving the action of wetting and adhesion. Such changes in the surface energy of the AOC after laser melting are due to the fact that HPDL melting of the surface of the AOC results in partial vitrification of the surface; a transition that is known to affect a reduction in γ_{sv} and an increase in γ_{sv}^p [26].

It is important to note that because of the long range ionic interactions in the AOC and the composite nature of the interfaces between the AOC and the liquids, it is very likely that the thermodynamically defined total solid surface energy, γ, as defined in Eq. (2), will be higher than the sum of the dispersive, γ^d, and the polar, γ^p, components of the surface energy. However, the increase in (excess) surface free energy will probably be less than the increase in the total lattice energy. On the other hand an absorbed liquid layer may shield the ionic fields substantially. As such, all the data derived from Eqs. (6)–(11) should be considered as being semi-empirical. Notwithstanding this, as the studies by Gutowski et al. [6] and Agathopoulos et al. [26] show, it is reasonable to conclude from the data obtained from Eqs. (6)–(11) that the HPDL treatment of the AOC surface has caused an increase in the polar component, γ^p, of the surface energy.

3.3. Influence of surface melting on wettability

It is important to determine the degree of laser treatment necessary to facilitate such surface energy changes. In particular, to establish what role melting, which is inherently influenced by the power density, of the AOC surface plays in the promotion of wetting. In order to analyse the effect melting of the AOC surface has on the wettability performance, a series of wetting experiments using the enamel were conducted to determine the contact angle for a range of power densities. The experiments were carried out with an O_2 shield gas at a traverse speed of 240 mm min^{-1}. The contact angle measurement procedure was as described in Section 3.2. The surface condition of the laser treated AOC was determined by means of SEM analysis. The relationship between the contact angle and the power density is shown in Fig. 7.
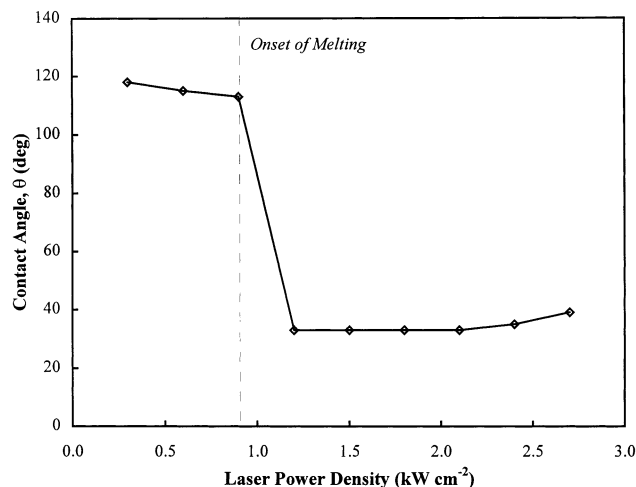

Fig. 7. Relationship between enamel contact angle on HPDL treated AOC and power density.
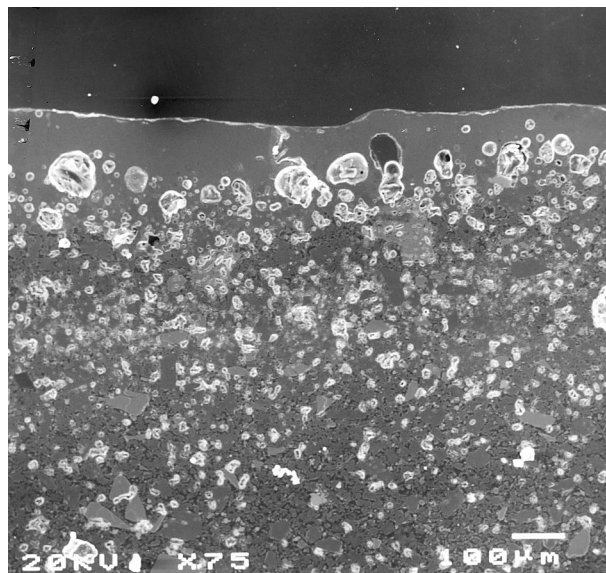

Fig. 8. Typical SEM cross-sectional images of the laser treated AOC.

As can be seen clearly from Fig. 7, the surface condition of the laser treated AOC has a significant effect on the contact angle. In particular, Fig. 7 indicates that the melting, and thus the partial vitrification of the glass forming elements (SiO_2 and Al_2O_3) within the AOC, is an essential prerequisite in order for significant reductions in the contact angle to be realised. As one can see, after the onset of melting at around 0.9 kW cm^{-2} the contact angle reduces sharply from 113 to 33°, after which no further decrease (or increase) is discernible until the power density exceeds 2.1 kW cm^{-2}. After this point a small increase in the contact angle from 33 to 39° was observed. This increase is probably due to the fact that this power density level lies outside of the optimum operating conditions for the traverse speed used in the experiments, and as such, will cause an increase in the surface roughness which, as was seen earlier, has a small but discernible effect on the contact angle. Furthermore, the melt depth observed within the region of the optimum operating conditions in which significant changes to the contact angle were achieved was measured as being from 50 to 125 μm. Fig. 8 shows a typical cross-section through the laser treated AOC, showing clearly the upper melted and densified layer. As can be seen from Fig. 8, as the depth from the melt layer increases, then the amount of densification gradually decreases. The mere reordering of the crystals that occurs at power densities below 0.9 kW cm^{-2} appears to have only a slight effect on the contact angle, reducing it from 118 to 113°. Nevertheless, such a reduction in the contact angle reveals that laser interaction without the incidence of melting does affect slightly the wettability characteristics of the AOC.

4. Conclusion

Laser surface melting of the AOC surface was necessary in order to allow the enamel to wet and adhere to the AOC surface. As such, the laser melting of the AOC surface resulted in the contact angle decreasing from 118 to 33°. Both the laser treatment of the AOC surface and the wettability experiments were conducted in normal atmospheric conditions. Wetting, and subsequent bonding, of the enamel to the AOC surface after laser melting was identified as being due to:

1. The laser melting of the AOC surface reducing the surface roughness from an Ra value of 25.9 µm before laser melting, to 6.3 µm after laser melting, thus directly reducing the contact angle θ.
2. The semi-empirically determined increase in the polar component of the surface energy γ_{sv}^{p}, (2.0 to 16.2 mJ m^{-2}) after laser melting as a result of the partial laser vitrification of the glass forming elements within the AOC composition, thus improving the action of wetting and adhesion.
3. The 36% increase in the surface oxygen content of the AOC resulting from laser melting was identified as further promoting the action of wetting.

This work demonstrates that it is possible to alter the wetting characteristics of the AOC using the HPDL to facilitate the firing of a vitreous enamel onto the AOC surface, a task not possible without laser melting. Moreover, the findings of this work show that with the use of laser radiation it is a distinct possibility that the wetting characteristics of many other materials could be altered.

Acknowledgements

References

[1] M. Ueki, M. Naka, I. Okamoto, J. Mater. Sci. Lett. 5 (1986) 1261–1262.
[2] P. Nikopoulos, D. Sotiropoulou, J. Mater. Sci. Lett. 6 (1987) 1429–1430.
[3] P.R. Chidambaram, G.R. Edwards, D.L. Olson, Mater. Trans. B 23 (1992) 215–222.
[4] J.G. Li, J. Mater. Sci. Lett. 11 (1992) 903–905.
[5] J.G. Li, Mater. Lett. 22 (1995) 169–174.
[6] V.W. Gutowski, L. Russell, A. Cerra, Adhesion of silicone sealants to organic-coated aluminium, in: J.M. Klosowski (Ed.), Science and Technology of Building Seals, Sealants, Glazing and Waterproofing, ASTM, Philadelphia, PA, 1992, pp. 144–159.
[7] X.B. Zhou, J.Th.M. De Hosson, J. de Phys. IV (3) (1993) 1007–1011.
[8] X.B. Zhou, J.Th.M. De Hosson, Acta Metall. Mater. 42 (1994) 1155–1162.
[9] J.G. Li, Rare Met. 2 (1993) 84–96.
[10] T. Bahners, W. Kesting, E. Schollmeyer, Appl. Surf. Sci. 69 (1993) 12–15.
[11] T. Bahners, Opt. Quan. Elec. 27 (1993) 1337–1348.
[12] J. Lawrence, L. Li, J.T. Spencer, in: Proceedings of ICALEO'96: Laser Materials Processing, Detroit, pp. 138–148.
[13] M.J. Jaycock, G.D. Parfitt, Chemistry of Interfaces, Wiley, Chichester, 1981, pp. 234–247.
[14] W.A. Zisman, Contact angle, wettability and adhesion, in: R.F. Gould (Ed.), Advances in Chemistry Series 43, American Chemical Society, Washington, DC, 1964, pp. 1–51.
[15] A.W. Neumann, Adv. Colloid Interf. Sci. 4 (1974) 438.
[16] F.M. Fowkes, Ind. Eng. Chem. 56 (1964) 40–52.
[17] E.P. DeGarmo, J.T. Black, R.A. Kohser, Materials and Processes in Manufacturing, Prentice-Hall, Englewood Cliffs, NJ, 1997, p. 379.
[18] L. Pennisi, Ceramics and glasses, in: S.J. Schneider (Ed.), Engineered Materials Handbook, ASM International, Metals Park, OH, 1991, pp. 255–259.
[19] L.S. O'Bannon, Dictionary of Ceramic Science and Engineering, Plenum, New York, 1984, p. 232.
[20] W.M. Steen, Laser Materials Processing, Springer, Berlin, 1991, p. 147.
[21] D.W. Richerson, Modern Ceramic Engineering, Marcel Dekker, New York, 1992, p. 217.
[22] T.Z. Kattamis, Laser in Metallurgy, AMIE, New York, 1981, p. 1.
[23] R.N Wenzel, Ind. Eng. Chem. 28 (1936) 988–994.
[24] A.B.D. Cassie, S. Baxter, Trans. Faraday Soc. 40 (1944) 546–552.
[25] X.B. Zhou, J.Th.M. De Hosson, J. Mater. Res. 10 (1995) 1984–1992.
[26] S. Agathopoulos, P. Nikolopoulos, J. Biomed. Mater. Res. 29 (1995) 421–429.
[27] D.L. Bourell, H.L. Marcus, J.W. Barlow, J.J. Beaman, Int. J. Powder Metall. 28 (1992) 369–381.
[28] M. Agarwala, D.L. Bourell, J.J. Beaman, H.L. Marcus, J.W. Barlow, Rapid Prototyping J. 1 (1995) 26–36.
[29] G. Nicolas, M. Autric, W. Marine, G.A. Shafeev, Appl. Surf. Sci. 109–110 (1997) 289–292.
[30] A. Feng, B.J. McCoy, Z.A. Munir, D. Cagliostro, Mater. Sci. Eng. A 1-2 (1998) 50–56.
[31] D.K. Chattoraj, K.S. Birdi, Adsorption and the Gibbs Surface Excess, Plenum, New York, 1984, p. 95.
[32] R.J. Good, L.A. Girifalco, J. Phys. Chem. 64 (1960) 561–565.